

Deep Explainable Relational Reinforcement Learning: A Neuro-Symbolic Approach

Rishi Hazra¹ ✉ and Luc De Raedt^{1,2}

¹ Centre for Applied Autonomous Sensor Systems (AASS),
Örebro University, Sweden

² Department of Computer Science, KU Leuven, Belgium
{rishi.hazra,luc.de-raedt}@oru.se

Abstract. Despite numerous successes in Deep Reinforcement Learning (DRL), the learned policies are not interpretable. Moreover, since DRL does not exploit symbolic relational representations, it has difficulties in coping with structural changes in its environment (such as increasing the number of objects). Relational Reinforcement Learning, on the other hand, inherits the relational representations from symbolic planning to learn reusable policies. However, it has so far been unable to scale up and exploit the power of deep neural networks. We propose Deep Explainable Relational Reinforcement Learning (DERRL), a framework that exploits the best of both – *neural* and *symbolic* worlds. By resorting to a neuro-symbolic approach, DERRL combines relational representations and constraints from symbolic planning with deep learning to extract interpretable policies. These policies are in the form of logical rules that explain how each decision (or action) is arrived at. Through several experiments, in setups like the Countdown Game, Blocks World, Gridworld, and Traffic, we show that the policies learned by DERRL can be applied to different configurations and contexts, hence generalizing to environmental modifications.

Keywords: Neuro-Symbolic AI · Relational Reinforcement Learning · Deep Reinforcement Learning, Explainability.

1 Introduction

Deep Reinforcement Learning (DRL) [2] has gained great success in many domains. However, so far, it has had limited success in relational domains, which are typically used in symbolic planning [40]. In the prototypical blocks world game (Figure 1), one goal is to place block *a* on block *b*. An obvious plan for achieving this is to *unstack* the blocks until both blocks *a* and *b* are at the top, upon which block *a* can be moved atop block *b*. Standard DRL approaches struggle to adapt to out-of-domain data, such as placing block *c* on *d*, or applying the learned strategies to changes in the stack size or the number of stacks, thus failing to

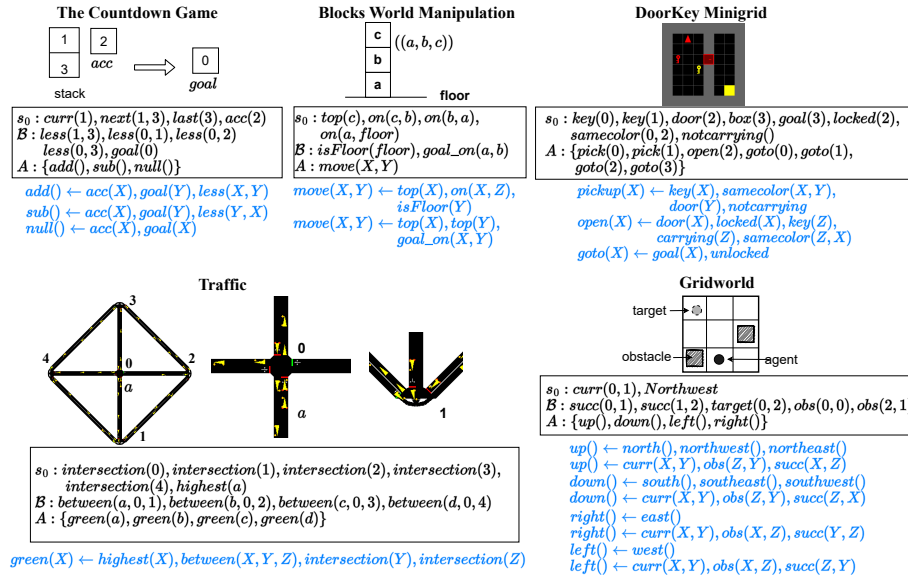


Fig. 1: Learned rules in all environments. [Row 1]left to right. Countdown Game: select operations (addition, subtraction, null) to make accumulated = target; Blocks World: place a specific block on another; DoorKey: unlock a door with a matching key to reach a goal. [Row 2] Traffic: minimize traffic at grid intersections. The figure shows a 5-agent grid with intersections 0 and 1 connected by lane a ; Gridworld: navigate a grid to reach the goal. Descriptions in Section 5.1.

learn generalized policies. Furthermore, the black-box nature of the learned policies makes it difficult to interpret action choices, especially in domains involving transparency and safety [33,47,22]. Understanding a machine’s decision-making is crucial for human operators to eliminate irrational reasoning [51,17].

Relational Reinforcement Learning (RRL) [7,49] combines symbolic planning and reinforcement learning and has origins in Statistical Relational AI and Inductive Logic Programming (ILP) [39,5]. RRL uses logic programs to represent interpretable policies that are similar to symbolic planning languages [11,16,15]. These policies use relations and objects, rather than specific states and actions, allowing agents to reason about their actions at a higher level of abstraction, and applying the learned knowledge to different situations. Earlier RRL approaches were purely symbolic [7,6,26,38], searching policy spaces guided by performance estimates, but did not exploit deep learning advancements and were not robust to noisy data. Recent approaches [56] use neural networks for scalability and improved internal representations, but learned policies are not human-readable.

We introduce **Deep Explainable Relational Reinforcement Learning (DERRL)**: neural DRL + symbolic RRL, a neuro-symbolic RRL approach that combines the strengths of neural (differentiability and representational power) and symbolic methods (generalizability and interpretability) while addressing their respective shortcomings. More specifically, DERRL uses a neural network to search

the space of policies represented using First-Order Logic (FOL)-based rules³. Like other ILP methods, our framework provides interpretable solutions. However, instead of using search-based methods, we leverage the representational capacity of neural networks to generate interpretations of actions (called rules), while entirely bypassing the need to interpret the network itself. To be specific, we propose a parameterized rule generation framework where a neural network learns to generate a set of generalized *discriminative* rules that are representations of the policy. For instance, as shown in the blocks world manipulation game in Figure 1, the two rules corresponding to *move* action are $move(X, Y) \leftarrow top(X), on(X, Z), isFloor(Y)$, which triggers an *unstacking* process, and $move(X, Y) \leftarrow top(X), top(Y), goal_on(X, Y)$, which puts block *a* on *b* when both are top blocks in the stacks. Note, that the same rules are applicable for a new goal (say $goal_on(c, d)$) or when blocks are increased to 10.

Additionally, we formulate a semantic loss [53] to guide the rule learning and restrict the hypothesis space of rules. This loss enforces semantic constraints on rule structure through a differentiable relaxation of semantic refinement [4] allowing users to encode background knowledge as axioms to mitigate rule redundancy. For example, in the rule $r \leftarrow less(X, Y), less(Y, Z), less(X, Z)$, due to the transitive relation $less(X, Z) \leftarrow less(X, Y), less(Y, Z)$, the term $less(X, Z)$ is redundant. DERRL enables predefining such knowledge as axioms, penalizing models that violate them. We compare our framework with that of Neural Logic Reinforcement Learning (NLRL) [25] which uses FOL to represent reinforcement learning policies and is based on Differentiable Inductive Logic Programming (∂ ILP) [10]. Much like DERRL, NLRL uses policy gradients to train a differentiable ILP module by assigning learnable weights to rules. The authors demonstrate interpretability and generalizability of policies to different problem configurations. We demonstrate DERRL’s advantages over NLRL in terms of computational efficiency, policy accuracy, and semantic constraint enforcement. **Contributions.** (i) A neuro-symbolic framework **DERRL** for learning interpretable RL policies in on-policy, model-free settings, demonstrating their adaptability to environmental changes; (ii) A differentiable relaxation of semantic refinement for guiding rule generation and constraining the hypothesis space.

2 Related Works

Integrating Symbolic Planning and RL. Recent research has sought to merge symbolic planning with deep reinforcement learning (DRL) to improve data efficiency and performance, as seen in works like PEORL [55], RePreL [30], and SDRL [36]. These approaches aim to integrate a high-level planner that suggests sub-goals to be executed by a low-level DRL model, thus relying on pre-defined environment dynamics, such as high-level action schemas with pre and postconditions. DERRL differs from planning-based methods as it is purely a RL approach, i.e. it does not have access to precise handcrafted action schemas or the

³ DERRL uses a relational representation akin to Quinlan’s FOIL[42] with background knowledge comprising ground facts and non-recursive Datalog-formulated rules.

reward function, and instead learns suitable control policies through trial-and-error interactions with the environment. Therefore, we only compare DERRL with other RL baselines. **Explainable RL.** Previous studies on interpretable RL have utilized decision trees for their ease of interpretation. Standard decision trees consist of nested if-then rules, are non-differentiable, and cannot be trained using gradient descent methods. The online nature of RL problems, combined with the non-stationarity introduced by an improving policy, presents additional challenges for decision trees as the agent interacts with the environment. One straightforward but inefficient solution is to re-learn the decision trees from scratch [8]. More recently, researchers have explored the use of differentiable functions in decision trees [12]. Differentiable Decision Trees have also been adapted for the RL framework [44,34], although their performance does not match that of deep neural networks. **Concurrent Works.** Our work on integrating differentiable logic programming into RL is concurrent with efforts such as NLRL [25] and dNL-ILP [41]. While dNL-ILP lacks goal generalization, we use the recent NLRL as our baseline. Recent research has also employed Graph Neural Networks [29] to capture relational representations [13,14] with applications to DRL [24] demonstrating zero-shot generalization to varying problem sizes. DERRL additionally learns interpretable policies. **Adjusting Language Bias** The possible hypothesis space expands exponentially with input space, necessitating user adjustments to language biases based on domain knowledge. Relational learning systems use declarative bias via semantic refinement [4]. Differentiable rule learning methods like ∂ ILP [10] and NLRL [25] use rule templates to limit rule body atoms to 2. However, these methods overlook background knowledge and face redundancies. DERRL mitigates redundancies and shrinks the search space through a differentiable relaxation of semantic refinement.

3 Preliminaries

3.1 Logic Programming:

Logic Programming [35] rules are written as **clauses** of the form $\alpha \leftarrow \alpha_1, \dots, \alpha_m$ composed of a **head** atom α and a **body** $\alpha_1, \dots, \alpha_m$. These clauses are defined using the standard *if-then* rules, wherein, if the body is satisfied, the head is true. Each **atom** is a tuple $p(v_1, \dots, v_n)$ where p is a n-ary **predicate** and v_1, \dots, v_n are either **variables** or **constants**. A **ground** atom is one that contains only constants. A predicate can either be **extensional** when it is defined by a set of ground atoms, or **target** (intensional) when it is defined by a set of clauses.

An **alphabet** \mathcal{L} is defined by the tuple $\mathcal{L} := (P_{\text{tar}}, P_{\text{ext}}, \text{arity}, C, V)$ where, P_{tar} is a set of target predicates, P_{ext} is a set of extensional predicates, $\text{arity} : P_{\text{ext}} \cup P_{\text{tar}} \mapsto \mathbb{N}$ is the number of arguments (variables or constants) that the predicate can take, C is a set of constants and V is a set of variables allowed in the clause. For the blocks world game in Figure 1, $P_{\text{tar}} = \{\text{move}/2\}$, $P_{\text{ext}} = \{\text{top}/1, \text{on}/2, \text{goal_on}/2, \text{isFloor}/1\}$, $V = \{X, Y, Z\}$, $C = \{a, b, c\}$.

3.2 Relational Markov Decision Process:

We model our problem as a Relational MDP (RMDP) given by the tuple $\mathcal{E} := (S, \mathcal{B}, A, \delta, r, \gamma)$ which is just like a regular MDP, but with relational states and actions. Here, S is a set of states, where each state is represented as a set of ground atoms consisting of predicates in P_{ext} and constants in C ; \mathcal{B} is the background knowledge also represented in form of ground atoms consisting of predicates and constants, but unlike the state, it remains fixed over the episode; A is a set of actions consisting of ground atoms from predicates in P_{tar} and constants in C ; $\delta : S \times A \mapsto S$ is an **unknown** transition function; $r : S \times A \mapsto R$ is an **unknown** real-valued reward function; γ is the discount factor. In the blocks world game (Figure 1), for the tuple $((a, b, c))^4$, the initial state s_0 and \mathcal{B} are $\{top(c), on(c, b), on(b, a), on(a, floor)\}$ and $\{isFloor(floor), goal_on(a, b)\}$, respectively. The actions are $move(X, Y)$ where variables X and Y can be substituted with constants in C . Although underlying models often use logical transition and reward rules [27], our approach is model-free, so we ignore them here.

3.3 Problem Statement:

Given, a tuple $(\mathcal{L}, \mathcal{E})$ where \mathcal{L} is an alphabet, and \mathcal{E} is an RMDP;

Find an optimal policy $\pi_\theta : S \cup \mathcal{B} \mapsto A$ as a set of clauses (also called **rules**) that maximizes the expected reward $\mathbb{E}_{\tau \sim \pi_\theta} [R_\tau]$, where $R_\tau := \sum_{k=t+1}^{T-1} \gamma^{k-t-1} R_k$. Here, an episode trajectory is denoted by τ .

More formally, the rules are selected from the hypotheses space, which is the set of all possible clauses. The head atom of each such rule is an action and the body is the definition of the action. As shown in Figure 1, a rule for $move(X, Y)$ in the blocks world environment is given as $move(X, Y) \leftarrow top(X), on(X, Z), isFloor(Y)$ which states that $move(X, Y)$ is triggered when the rule definition (i.e., the body) is satisfied. Thus, if the policy selects the action $move(c, floor)$, one can quickly inspect the body to find out **how** that action was taken. The rules are *discriminative* (i.e. that help select the correct action by distinguishing it from alternative actions) and together provide an interpretation of the policy. A set of rules is learned for each action. Once trained, the rules for actions do not change and the rule body decides which action should be triggered at each time-step. In what follows, we provide a detailed explanation of rule generation and inference for each time-step of an episode. For simplicity, we expunge the time-step notation (for e.g., state at t^{th} time-step s_t is now s).

4 Proposed Approach

Consider an alphabet \mathcal{L} where $P_{\text{tar}} = \{r/0, s/0\}$, $P_{\text{ext}} = \{p/1, q/2\}$, $V = \{X, Y\}$, $C = \{a, b\}$. The set of all ground atoms G formed from the predicates in P_{ext} and

⁴ Here, the outer tuple denotes stacks and the inner tuples denote the blocks in the stack. For e.g., $((a, b), (c, d))$ has two stacks: (a, b) is stack 1 and (c, d) is stack 2.

constants in C is $\{p(a), p(b), q(a, a), q(a, b), q(b, a), q(b, b)\}$. We represent each ground atom $g_j \in G$ along with its index j in Table 1.

Recall, that both state s and background knowledge \mathcal{B} are represented using ground atoms. Given a state $s = \{p(a), q(a, a), q(a, b)\}$ at each time-step, and an empty background knowledge \mathcal{B} , we encode it to a state vector \mathbf{v} , such that each element $v_j = 1$ if $g_j \in \{s, \mathcal{B}\}$ (i.e. if the current state s or the background knowledge \mathcal{B} contains the ground atom g_j), else 0. Let us now consider the set of all atoms K formed from the predicates in P_{ext} and variables in V (instead of the constants in C). Table 2 lists the atoms $k_j \in K$ and the corresponding \mathbf{v} .

Table 1: Table of all ground atoms G and their indices j .

j	0	1	2	3	4	5	
g_j	$\mathbf{p}(\mathbf{a})$	$p(b)$	$\mathbf{q}(\mathbf{a}, \mathbf{a})$	$\mathbf{q}(\mathbf{a}, \mathbf{b})$	$q(b, a)$	$q(b, b)$	$s = \{p(a), q(a, a), q(a, b)\}$
v_j	1	0	1	1	0	0	$\mathbf{v} = [1, 0, 1, 1, 0, 0]$

Table 2: All atoms K , their indices j , the generated rule vectors $\mathbf{b}^r, \mathbf{b}^s$, and corresponding probability vectors $\mathbf{P}^r, \mathbf{P}^s$ for target actions $P_{\text{tar}} = r/0, s/0$.

j	0	1	2	3	4	5	
k_j	$p(X)$	$p(Y)$	$q(X, X)$	$q(X, Y)$	$q(Y, X)$	$q(Y, Y)$	
\mathbf{b}_j^r	0	1	0	0	1	0	$r \leftarrow p(Y), q(Y, X)$
\mathbf{P}_j^r	0.1	0.8	0.3	0.4	0.7	0.2	$\mathbf{w}^r = [0.8, 0.7]^\top$
\mathbf{b}_j^s	1	0	0	0	0	1	$s \leftarrow p(X), q(Y, Y)$
\mathbf{P}_j^s	0.6	0.3	0.4	0.2	0.1	0.9	$\mathbf{w}^s = [0.6, 0.9]^\top$

We represent rules using rule vectors. As shown in Table 2, the rule vector for each action $i \in A$ is given as $\mathbf{b}^i \in \{0, 1\}^m$, where $m = |K|$ (i.e. the cardinality of the set of all atoms formed from the predicates in P_{ext} and variables in V). Here, $b_j^i = 1$, if the j^{th} atom is in the body of the i^{th} rule. From Table 2, $\mathbf{b}^r = [0, 1, 0, 0, 1, 0]^\top$ corresponds to the rule $r \leftarrow p(Y), q(Y, X)$.

We impose the Object Identity (OI) assumption [28] which states that during grounding and unification, distinct variables must be mapped to distinct constants. For instance, ground rules for $r \leftarrow p(Y), q(Y, X)$ are $r \leftarrow p(b), q(b, a)$ and $r \leftarrow p(a), q(a, b)$ under substitutions $\phi_0 = \{a/X, b/Y\}$ and $\phi_1 = \{b/X, a/Y\}$, respectively, but a substitution $\phi_2 = \{a/X, a/Y\}$ is not allowed. Without loss of generality, one can model nullary predicates and negated atoms, by simply including additional dimensions (corresponding to atoms in K) in the vector \mathbf{b}^i .

The DERRL framework learns a rule vector \mathbf{b}^i for each action $i \in A$ by associating it with a trainable weight vector \mathbf{w}^i . Each element $w_j^i \in \mathbf{w}^i$ indicates the membership of the corresponding atom in the rule definition (i.e., if the weight of the atom is high, it is more likely to belong to the rule definition). Given the state vector \mathbf{v} , action probabilities $\pi_\theta(i | s, \mathcal{B})$ are calculated by performing a fuzzy conjunction on the rules (Section 4.2). The whole framework is trained end-to-end using the REINFORCE algorithm [52], with the loss function given as

$J(\pi_\theta) = -\mathbb{E}_{\tau \sim \pi_\theta} [R_\tau]$. Here, R_τ is the discounted sum of rewards over trajectory τ , and θ is the set of trainable parameters.

Algorithm 1 summarizes the DERRL framework. The two main components of DERRL are **(i)** Rule Generator (Section 4.1), which at every time-step t and for each action $i \in A$, generates a rule vector \mathbf{b}^i , and a weight vector \mathbf{w}^i ; **(ii)** Forward chaining Inference (Section 4.2) that takes the generated rules vectors for all actions $\{\mathbf{b}^i\}_{i=1}^{|A|}$, the corresponding weight vectors $\{\mathbf{w}^i\}_{i=1}^{|A|}$, and the state valuation vector \mathbf{v} for the t^{th} time-step, and returns the action probabilities $\pi_\theta(\cdot | s, \mathcal{B})$. Note, that the rule generator parameters θ are trained by calculating the gradients of the loss function with respect to weight vectors \mathbf{w}^i .

4.1 Rule Generation

The rule $\mathcal{R}_\theta : i \mapsto \mathbf{b}^i, \mathbf{w}^i$ uses a parameterized network \mathcal{R}_θ to map each action (index) i to a rule vector \mathbf{b}^i and weight vector \mathbf{w}^i . Here, $b_j^i = 1$ indicates the j^{th} atom is in the rule body. The rule generator outputs a probability vector \mathbf{P}^i where P_j^i represents the probability of the j^{th} atom in K belonging to the rule body. We use the Gumbel-max trick [23] on \mathbf{P}^i to sample the binary vector \mathbf{b}^i .

$$b_j^i = \arg \max(\log(P_j^i) + u_0, \log(1 - P_j^i) + u_1) \text{ where } u \sim \text{Gumbel}(0, 1)$$

Here, $\text{Gumbel}(0, 1)$ is the standard Gumbel distribution given by the probability density function $f(x) = e^{-(x+e^{-x})}$. During evaluation, we use $\arg \max(\cdot)$ operation without sampling. From \mathbf{P}^i , we also obtain the weight vector $\mathbf{w}^i \in \mathbb{R}^{\|\mathbf{b}^i\|_1}$ comprising the probabilities of only those atoms which have $b_j^i = 1$. From Table 2, the generated rule vector $\mathbf{b}^r = [0, 1, 0, 0, 1, 0]^\top$, the probability vector $\mathbf{P}^r = [0.1, 0.8, 0.3, 0.4, 0.7, 0.2]^\top$, and the corresponding weight vector $\mathbf{w}^r = [0.8, 0.7]^\top$.

4.2 Inference

i	\mathbf{X}^i	\mathbf{Y}^i	\mathbf{w}^i	\mathbf{z}^i	\mathcal{F}^i	$\pi_\theta(i s, \mathcal{B})$
$r \leftarrow p(Y), q(Y, X)$	$\begin{bmatrix} 0, 3 \\ 1, 4 \end{bmatrix}$	$\begin{bmatrix} 1, 1 \\ 0, 0 \end{bmatrix}$	$\begin{bmatrix} 0.8 \\ 0.7 \end{bmatrix}$	$\begin{bmatrix} 0.5 \\ 0 \end{bmatrix}$	0.5	0.62
$s \leftarrow p(X), q(Y, Y)$	$\begin{bmatrix} 0, 5 \\ 1, 2 \end{bmatrix}$	$\begin{bmatrix} 1, 0 \\ 0, 1 \end{bmatrix}$	$\begin{bmatrix} 0.6 \\ 0.9 \end{bmatrix}$	$\begin{bmatrix} 0 \\ 0 \end{bmatrix}$	0	0.38

Consider the following rules generated by the rule generator. Each rule is passed through a substitution $\phi : V \mapsto C$ to produce ground rules. Let, $\mathbf{X}^i \in \mathbb{Z}_{\geq 0}^{N(\phi) \times \|\mathbf{b}^i\|_1}$ be the matrix representation of the ground rules. Here, $\mathbb{Z}_{\geq 0}$ and $N(\phi)$ are the set of non-negative integers and the number of possible substitutions, respectively. Each row in \mathbf{X}^i is a vector of ground atom indices that belong to the ground rules. Using a substitution $\phi = \{b/X, a/Y\}$, we obtain the ground rule $r \leftarrow p(a), q(a, b)$. From Table 1, this rule definition can be written as the vector $[0, 3]$ (i.e., indices of $p(a)$ and $q(a, b)$ are 0, 3, respectively). Similarly, the substitution $\phi = \{a/X, b/Y\}$ gives us $r \leftarrow p(b), q(b, a)$, and the vector $[1, 4]$.

Next, the $\text{value}(\cdot)$ operation takes each element \mathbf{X}_j^i and returns its state value v_j . From Table 1, $\mathbf{Y}^r = \text{value}(\mathbf{X}^r) = \text{value}\left(\begin{bmatrix} 0, 3 \\ 1, 4 \end{bmatrix}\right) = \begin{bmatrix} v_0, v_3 \\ v_1, v_4 \end{bmatrix} = \begin{bmatrix} 1, 1 \\ 0, 0 \end{bmatrix}$. The row vectors of $\mathbf{Y}^i = [\mathbf{y}_1^i, \dots, \mathbf{y}_{N(\phi)}^i] \in \mathbb{R}^{N(\phi) \times \|\mathbf{b}^i\|_1}$ can be regarded as truth values of the grounded rule (i.e., for each substitution ϕ), based on $\{s, \mathcal{B}\}$. If the rule definition is not satisfied, the corresponding row vectors will have sparse entries. To ensure differentiability, we use fuzzy norms for our rules.

Fuzzy Conjunction Operators. Fuzzy norms integrate logic reasoning with deep learning by approximating the truth values of predicates [10,37]. Fuzzy conjunction operators $* : [0, 1]^{\|\mathbf{b}^i\|_1} \mapsto [0, 1]$ can be of various types like Godel t-norm and Product t-norm (refer Section 11). We use Lukasiewicz t-norm ($\top_{\text{Luk}}(a, b) := \max\{0, a + b - 1\}$) to compute the action values for each rule⁵. To encourage the rule generator to generate more precise rules with higher probability, we calculate a valuation vector by weighing each row $\mathbf{y}_k^i \in \mathbb{R}^{\|\mathbf{b}^i\|_1}$ with the weight vector $\mathbf{w}^i \in \mathbb{R}^{\|\mathbf{b}^i\|_1}$, and using the Lukasiewicz operator as $z_k^i = \max(0, \langle \mathbf{y}_k^i, \mathbf{w}^i \rangle - \|\mathbf{w}^i\|_1 + 1)$. Intuitively, the inner product $\langle \mathbf{y}_k^i, \mathbf{w}^i \rangle$ is a weighted sum over all atoms in the rule body that are true in $s \cup \mathcal{B}$. This is akin to performing $(a + b)$ in t-norm operator. For $\mathbf{y}_0^r = [1, 1]^\top$, $\mathbf{w}^r = [0.8, 0.7]$:

$$z_0^r = \max(0, \langle \begin{bmatrix} 1 \\ 1 \end{bmatrix}, \begin{bmatrix} 0.8 \\ 0.7 \end{bmatrix} \rangle - 1) = 0.5$$

With multiple substitutions (or groundings) for a generated rule, we find the maximum valuation as $\mathcal{F}^i = \max(\mathbf{z}^i)$. The final action probability is calculated as $\pi_\theta(i | s, \mathcal{B}) = \text{softmax}(\mathcal{F}^i)$. Note, that if the generated rule is not satisfied for any substitution (i.e., has a sparse row vector in the matrix \mathbf{Y}^i), the valuation of the generated rule is lower (for e.g., from the above table $\mathcal{F}^s < \mathcal{F}^r$).

Multiple rules for a single action. We generalize DERRL to learn policies with multiple rules for each action, allowing it to switch between rules based on input (for e.g. in the blocks world game, the "move" action uses two rules executed at different steps depending on the goal blocks' position). We allow multiple rule networks per action, adjusting the final computation step to determine action probabilities based on the best-satisfied rule. Given \mathcal{F}_1^i and \mathcal{F}_2^i for two different rules for the same action, we first compute $\tilde{\mathcal{F}}^i = \max(\mathcal{F}_1^i, \mathcal{F}_2^i)$ to determine which rule is more appropriate at a given time-step. Consider two different rules generated for action r with arbitrary \mathbf{Y}^i :

⁵ More generally, given a vector $\mathbf{y} \in [0, 1]^n$, Lukasiewicz t-norm $\top_{\text{Luk}}\mathbf{y} := \max(0, \langle \mathbf{y}, \mathbf{1} \rangle - n + 1)$. For the proof, refer Section 11.

Algorithm 1 Deep Explainable Relational Reinforcement Learning (DERRL)**Input:** Alphabet: \mathcal{L} , RMDP: \mathcal{E} **Output:** (set of) rules that encode the policy π_θ Initialize rule generator parameters θ

```

for each episode do
  for  $t = 0$  to  $T - 1$  do
     $\mathbf{v} = \text{encode}(s, \mathcal{B})$  ▷ state vector
    for each action  $i$  do
       $\mathbf{b}^i, \mathbf{w}^i \sim \mathcal{R}_\theta(i)$  ▷ Rule Generation (Section 4.1)
    end for
     $\pi_\theta(\cdot | s, \mathcal{B}) = \text{Inference}(\mathbf{v}, \{\mathbf{b}^i\}_{i=1}^{|\mathcal{A}|}, \{\mathbf{w}^i\}_{i=1}^{|\mathcal{A}|})$  ▷ (Section 4.2)
     $a \sim \pi_\theta(\cdot | s, \mathcal{B})$ 
     $s' \leftarrow \delta(s, a); \quad R_t \leftarrow r(s, a)$ 
  end for
   $R_\tau \leftarrow \sum_{t+1}^{T-1} \gamma^{k-t-1} R_k$ 
   $\theta \leftarrow \theta - \eta \nabla_\theta \mathbb{E}_{\tau \sim \pi_\theta} [R_\tau]$ 
end for

```

i	\mathbf{Y}^i	\mathbf{w}^i	\mathbf{z}^i	\mathcal{F}^i
$r_1 \leftarrow p(Y), q(Y, X)$	$\begin{bmatrix} 1, 1 \\ 0, 0 \end{bmatrix}$	$\begin{bmatrix} 0.8 \\ 0.7 \end{bmatrix}$	$\begin{bmatrix} 0.5 \\ 0 \end{bmatrix}$	0.5
$r_2 \leftarrow p(X), p(Y), q(X, X)$	$\begin{bmatrix} 1, 0, 1 \\ 0, 1, 1 \end{bmatrix}$	$\begin{bmatrix} 0.6 \\ 0.8 \\ 0.8 \end{bmatrix}$	$\begin{bmatrix} 0 \\ 0 \\ 0 \end{bmatrix}$	0

Here, $\tilde{\mathcal{F}}^r = \max(0.5, 0) = 0.5$ is the valuation for rule r . Intuitively, depending on the current state s and background knowledge \mathcal{B} , one of the rules will be more appropriate (i.e., lower sparsity in rows of \mathbf{Y}^i) than the others, prompting the policy to switch to that rule for decision making⁶.

4.3 Semantic Constraints

The set of possible rules to consider grows exponentially with the number of predicates and their arity. While traditional relational learning systems have used declarative bias in form of semantic refinement [4], prior works in differentiable rule learning [10,25] employ rule templates to restrict the hypothesis space (e.g. rules of size 2). However, these methods frequently encounter redundancies. For example, rules $r \leftarrow \text{less}(X, Y), \text{less}(Y, Z), \text{less}(X, Z)$ and $s \leftarrow \text{equal}(X, Y), \text{equal}(Y, X)$ exhibit transitive and symmetric relations, respectively, making some atoms redundant. A rule r is redundant w.r.t. a constraint $h \leftarrow b_1, \dots, b_n$ if the rule $\text{false} \leftarrow h, b_1, \dots, b_n$ subsumes the rule r . To avoid redundancies, generated rule vectors with $b_j^i = 1$ for both atoms

⁶ This assumes a specified upper bound on the number of rules for each action, similar to selecting the number of clusters in a clustering algorithm [54].

$equal(X, Y)$ and $equal(Y, X)$ should be penalized. To this end, we propose a differentiable relaxation of semantic refinement by applying a supervised loss on probability vectors $\{\mathbf{P}^i\}_{i=1}^{|A|}$. We declare semantic constraints \mathcal{S}_c as axioms which can either be a relation (symmetric or transitive), or some background fact (like $false \leftarrow on(X, Y), on(Y, X)$). Then we calculate the semantic loss as $\mathcal{L}_{sem} = \sum_{x \in \mathcal{S}_c} \sum_{i \in A} \prod_{j \in x} P_j^i$.

Here, the outer summation is over each semantic constraint $x \in \mathcal{S}_c$, and the inner summation is over each generated rule $i \in A$. The product is over the probability of each atom (with index j) in the body of axiom x . For instance, given a single axiom $false \leftarrow p(Y), q(Y, X)$, for the generated rule $r \leftarrow p(Y), q(Y, X)$, from Table 2, the loss is $\mathcal{L}_{sem} = P_1^i \times P_4^i = 0.56$. Here, the loss is high because according to the given constraint, $p(Y)$ and $q(Y, X)$ should not appear together in the body of the rule. Intuitively, the loss is highest if the membership probabilities of both atoms are high warranting a penalization. \mathcal{L}_{sem} is summed over the entire episode and the final loss is given as $\bar{J}(\pi_\theta) = J(\pi_\theta) + \lambda_{sem} \mathcal{L}_{sem}$. Here, λ_{sem} is a regularization term. See Appendix 8 for constraints in all environments.

5 Experiments

Through our experiments, we aim to answer the following questions: (1) Can the proposed approach learn interpretable policies while performing on par with neural-based baselines? (Section 6.1); (2) Are the learned rules agnostic to modifications in the environment? (Section 6.2); (3) How efficient and scalable is the proposed approach compared to the current state-of-the-art NLRL? (Section 6.3)

5.1 Experimental Setup

The Countdown Game. The agent manipulates a stack of numbers and an initial accumulated value $acc(X)$ to match a target number $goal(X)$ by applying operations like addition (*add*), subtraction (*sub*), or no operation (*null*). The stack comprises of the top number ($curr(X)$), number below it ($next(X, Y)$), and bottom-most number ($last(X)$). From Figure 1, the state s_t includes the stack, accumulated number, and goal number. Operations are performed between the accumulated value and the top number of the stack⁷. The background knowledge \mathcal{B} comprises the target number⁸, and atoms of the form $less(X, Y)$ which denote that number X is less than Y . A reward of $r = 1$ is given when the target and accumulated values match at the end of the episode, otherwise $r = -\frac{|goal-acc|}{N_1}$ where N_1 is a normalizing constant. An initial range of numbers $[-4, 6]$ and stack of length= 2 is used for training. The learned models are tested for generalization on the following tasks (i) dynamic stack lengths of $\{3, 4, 5\}$; (ii) held-out target unseen during training; (iii) held-out initial stack sequences. We also train a stochastic game version with 10% probability of altering an action to null.

⁷ *add*: $acc += top$, *sub*: $acc -= top$, *null*: acc

⁸ $goal(X)$ is provided as background since it does not change during the episode.

Blocks World Manipulation. Given an initial configuration of blocks, the goal is to put a specified block atop another specified block (Figure 1). Stacks are represented using predicates: $top(X)$ means that block X is the top block, $on(X, Y)$ means that block X is on top of block Y . The actions are $move(X, Y)$ with $X = \{a, b, c\}$ and $Y = \{a, b, c, floor\}$. A reward $r = 1$ is provided if the task is achieved. To enforce optimal planning, we impose a penalty of $r = -0.02$ for every action. Training includes a fixed number of blocks = 3 and a fixed goal – to stack block a on block b ($goal_on(a, b)$). We train it with initial configurations: $((a, b, c)); ((c, a, b)); ((a, c), (b)); ((b, c), (a))$. Here, each tuple is a stack. For generalization, we use variations like (i) held-out configuration unseen during training like $((a, b), (c)); ((b, c, a)); ((b, a, c));$ (ii) dynamic (number of) blocks $\{4, 5\}$; (iii) dynamic (number of) stacks $\{2, 3, 4\}$; (iv) unseen goals like $goal_on(b, a)$ and $goal_on(a, c)$.

Gridworld. The agent navigates a grid with obstacles to reach the goal (Figure 1). The agent can move vertically ($up/down$) or sideways ($left/right$). The state information consists of the current position of the agent $curr(X, Y)$ where X and Y are the coordinates, and the compass direction of the target ($North, South, East, West, Northeast, Northwest, Southeast, Southwest$). The background information consists of target coordinates ($target(X, Y)$), obstacle coordinates ($obs(X, Y)$), and successor information $succ(X, Y)$ where $Y = X + 1$. The action space is $\{up, down, left, right\}$. The agent receives a reward of $r = 1$ for reaching the target, otherwise $r = -\frac{\|position_{goal} - position_{agent}\|_2}{N_2}$. Here N_2 is a normalizing constant. During training, a fixed size grid of 3×3 and 5×5 is used with the number of obstacles being fixed = 2. For generalization, we use the following variations: (i) dynamic (number of) obstacles $\{3, 4\}$; (ii) held-out (agent-goal) configurations. Unlike graph search algorithms like A* that assume access to the dynamics model, DERRL learns actions through exploration.

Traffic. We used the Simulation of Urban MObility (SUMO) traffic simulator [31] to simulate traffic flow, where intersections (3-way and 4-way) function as agents denoted by $intersection(Y)$, and are connected by a network of 2-way lanes represented as $between(X, Y, Z)$, indicating a connection between intersections Y and Z by lane X . The goal is to minimize the traffic at the intersections, hence reward is the negative queue length at each intersection. Each agent is provided with the lane that has the highest traffic, labeled as $highest(X)$ for lane X , and is responsible for controlling the traffic lights for that lane, enabling them to turn the lights green ($green(X)$) for a specific lane X . Therefore, 3 and 4-way intersections have an action space of size 3, 4 respectively. Although only two models (one for all 3-way intersections and another for all 4-way intersections) suffice, we train each intersection independently to demonstrate the scalability of DERRL to multi-agent setups, and also for future developments in cooperative multi-agent setups [57, 21]. We train on a grid comprising 5 agents and transfer the learned rules to an 8-agent grid. We show the mean rewards of all agents in Table 3 – note, that the best possible reward ≈ 0 .

DoorKey Minigrad. The agent task is to unlock a locked door ($locked(Y)$, $door(Y)$) and reach a goal ($goal(Z)$). Various colored keys ($key(X)$) are scattered

Table 3: Generalization Scores (average rewards over 50 episodes across 3 runs) compare DERRL to other baselines. DERRL outperforms baselines, including the state-of-the-art NLRL. In Traffic, the mean reward for all agents is reported.

Setup		DERRL	NLRL	GCN	MLP	Random
Countdown Game	training	0.98	0.95	0.98	1.00	0.30
	dynamic stack	0.98	0.95	0.95	0.54	0.38
	held-out target	0.98	0.85	0.95	0.35	0.33
	held-out initial	0.98	0.55	1.00	0.35	0.18
Countdown Game(stochastic)	training	0.98	0.95	0.98	1.00	0.15
Blocks World Manipulation	training	0.97	0.97	0.97	0.97	-0.18
	held-out config.	0.97	0.70	0.55	0.45	-0.18
	dynamic blocks	0.92	0.51	-0.20	-0.21	-0.22
	dynamic stacks	0.96	0.90	0.90	0.85	-0.18
	unseen goal	0.96	0.45	-0.18	-0.18	-0.18
DoorKey Minigrid	training	0.80	0.45	0.75	0.90	0.10
	dynamic keys/doors	0.78	0.25	0.35	0.20	0.05
Traffic	training (5-agents)	-0.76	-0.91	-0.90	-0.95	-1.54
	8-agents	-1.02	-1.28	-1.45	-1.75	-2.17
Gridworld Game	training	0.75	0.72	0.70	0.81	0.03
	dynamic obstacles	0.70	0.55	0.46	0.51	-0.15
	held-out config.	0.81	0.70	0.17	-0.61	-0.70

throughout the room, and the agent must select the key that matches the color of the door ($samecolor(X, Y)$) to unlock it. We use high-level actions. The agent is only allowed to carry one key at a time and can navigate to and pick up a key X using the $pick(X)$ action if it is not carrying any keys ($notcarrying$), otherwise, it drops the key before picking the new one. The $open(X)$ action enables it to unlock a door X if it carries the key that matches the door’s color. The $goto(X)$ action enables the agent to navigate to a specific object X . The reward = 1 for successfully reaching the goal, else 0. The learned model is tested for generalization with additional doors and keys of varying colors.

We evaluate our DERRL against Neural Logic Reinforcement Learning (**NLRL**) baseline. We also compare with model-free DRL approaches with variations in the deep learning module like (i) Graph Convolution Network (**GCN**) [29] that perform well at relational learning [32], and are invariant to the number of nodes in the graph; (ii) Multilayer Perceptron (**MLP**). Finally, we compare with a Random (**Random**) baseline where the weights of the MLP are randomized to set a lower limit on the performance. We use a single-layer neural network for our rule generator ($2m$ parameters). For the GCN and MLP baselines, we experimented with 2-layer networks ($O(m^3)$ parameters).

6 Results

6.1 Interpretation of policies (Q1)

In this section, we provide interpretations of the learned rules in each training environment, as shown in Figure 1. **The Countdown Game.** The policy selects *add* action when $acc(X) < goal(Y)$, *sub* action when $acc(X) > goal(Y)$, and null action when both are equal. **Blocks World Manipulation.** The policy learns two rules for $move(X, Y)$. Given a goal to put block a atop block b , the first rule is applicable when at least one of the blocks is not the top block. Hence, the policy learns to unstack the blocks – the top block X of the stack is moved to the floor Y . The second rule is applied when both a and b are at the top. **Traffic.** The general rule for each intersection is $green(X) \leftarrow highest(X), between(X, Y, Z), intersection(Y), intersection(Z)$. Intuitively, the lights corresponding to the lane with the highest traffic X , connecting intersections Y and Z , are turned green. **DoorKey Minigrid.** The learned rule for action $pickup(X)$ tells the agent to pickup the key X that matches the color of the door Y , provided that it is not carrying any other items (*notcarrying*). Similarly, for $open(X)$, the learned rule states that the agent can unlock a locked door X using the key Y only if the colors of the door and the key match. The $goto(X)$ action directs the agent to navigate to the goal object X when the door is *unlocked*. **Gridworld Game.** In this setting, the policy learns two rules for each action. The first is used for navigation to the target, such as moving *up* if the target is to the north (or northeast and northwest) of the grid. The second helps navigate around obstacles, e.g. move *up* if the obstacle (given by (Z, Y)) is to the immediate right of the agent (given by (X, Y)). However, the policy may not follow the shortest path⁹ or have consistent traversal strategies, resulting in varied rules for different instances without performance loss.

DERRL also bears similarities with Program Synthesis [48,3,20], which involves finding a program that meets user specifications and constraints. Learned policies can be rewritten as programs (see Appendix 10). For example, a program to solve the countdown game involves operating on current and accumulated values (using *add*, *sub*, *null* operations) until accumulated value = goal value.

6.2 Generalization performance (Q2)

From Table 3, we observe that DERRL learns general rules, generalizing to environment modifications, and outperforms baselines in generalization tasks. Unlike symbolic planning, DERRL’s performance remains unaffected by noisy training, such as stochastic Countdown. Secondly, although GCNs perform well in relational learning, their generalization is marginally better than MLP, potentially failing to capture task agnostic relational patterns. However, GCN surpasses MLP and NLRL in the countdown game. Lastly, DERRL’s training performance

⁹ When the target is to the southeast, and the agent encounters a target to its right, it will travel north (*up*) rather than south (*down*).

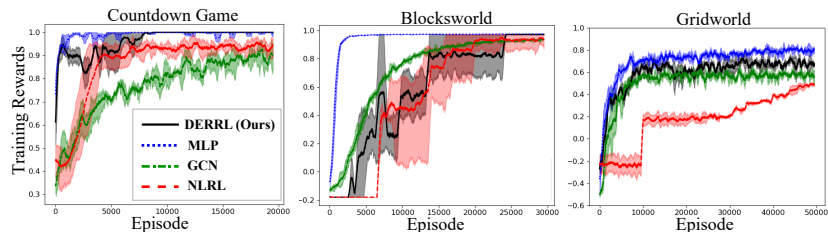


Fig. 2: [Best viewed in color] Comparison of training rewards at convergence for different baselines plotted by averaging the rewards over 3 independent runs. [Left to right] Countdown Game, Blocks World, and Gridworld.

is comparable to MLP, but it outperforms MLP in generalization tasks, where MLP is similar to the Random baseline. Additionally, DERRL’s convergence speed is on par with MLP, as shown in Figure 2.

6.3 Comparison with NLRL (Q3)

Computational Complexity. NLRL assigns trainable weights to all possible rules with a body size of 2, while DERRL allocates weights to each atom in the rule body. Given, m atoms from P_{ext} and V , NLRL has $C(m,2)$ learnable weights, while DERRL has $2m$. Therefore, the training reduces from learning the best set of rules (in NLRL) to learning the best membership of the rules (in DERRL), leading to a lower computation time in DERRL. The computation time per episode is reduced by a factor of ≈ 10 (Figure 3).

Comparing Learned Rules. NLRL learned rules in blocksworld are:

$$\begin{aligned} \text{move}(X, Y) &\leftarrow \text{top}(X), \text{pred}(X, Y); & \text{move}(X, Y) &\leftarrow \text{top}(X), \text{goal_on}(X, Y) \\ \text{pred}(X, Y) &\leftarrow \text{isFloor}(Y), \text{pred2}(X); & \text{pred2}(X) &\leftarrow \text{on}(X, Y), \text{on}(Y, Z) \end{aligned}$$

With invented predicates pred and pred2 , this plan differs from DERRL in that the second rule doesn’t verify if both X and Y are movable, failing to solve configurations where block b is below block a . **Size of hypothesis space.** DERRL restricts the hypothesis space through the use of semantic constraints in the optimization problem, whereas large hypothesis space in NLRL limits its convergence in DoorKey and Traffic domains. The convergence in DERRL is slower without semantic constraints (see Appendix 9 for ablations on DERRL with and without semantic constraints). **Expressiveness.** NLRL can learn recursive rules by using templates as in meta-interpretive learning and predicate invention. While this is expressive, it can be hard to master. In contrast, DERRL learns non-recursive Datalog as Quinlan’s FOIL [42] but combines it with constraints that can be recursive to rule out redundancies.

7 Conclusion

We proposed a neuro-symbolic approach to learn interpretable policies that are also generalizable. The representations that DERRL and RRL use are very sim-

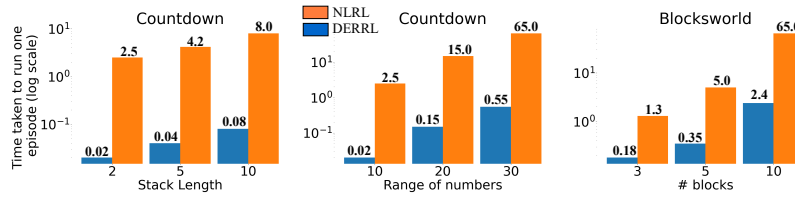


Fig. 3: Run-time comparison per episode between DERRL and NLRL as problems scale. Left to right: Countdown game (stack size), Countdown game (range of numbers), Blocks World (number of blocks). Y-axis in log scale. Plots show NLRL takes approximately 10 times longer per episode compared to DERRL. See additional plots in Appendix 9.

ilar to those used in the planning community. We also significantly improve upon the scalability of existing state-of-the-art NLRL. Upgrading the approach to enable automatic learning of the required number of rules can be a potential research direction. Also, as a part of future work, it will be interesting to explore ways in which the proposed approach can be scaled to real-life applications requiring the need to process raw sensory inputs.

Acknowledgement

This work was partially supported by the Wallenberg AI, Autonomous Systems and Software Program (WASP) funded by the Knut and Alice Wallenberg Foundation.

References

1. Alur, R., Bodik, R., Juniwal, G., Martin, M.M.K., Raghathan, M., Seshia, S.A., Singh, R., Solar-Lezama, A., Torlak, E., Udupa, A.: Syntax-guided synthesis. In: 2013 Formal Methods in Computer-Aided Design. pp. 1–8 (2013), <https://ieeexplore.ieee.org/document/6679385>
2. Arulkumaran, K., Deisenroth, M.P., Brundage, M., Bharath, A.A.: Deep reinforcement learning: A brief survey. *IEEE Signal Processing Magazine* **34**(6), 26–38 (2017)
3. Biermann, A.W.: The inference of regular lisp programs from examples. *IEEE Transactions on Systems, Man, and Cybernetics* **8**(8), 585–600 (1978), <https://ieeexplore.ieee.org/document/4310035>
4. De Raedt, L.: Logical and relational learning. In: Zaverucha, G., da Costa, A.L. (eds.) *Advances in Artificial Intelligence - SBIA 2008*. pp. 1–1. Springer Berlin Heidelberg, Berlin, Heidelberg (2008)
5. De Raedt, L., Kersting, K., Natarajan, S., Poole, D.: *Statistical Relational Artificial Intelligence: Logic, Probability, and Computation, Synthesis Lectures on Artificial Intelligence and Machine Learning*, vol. 32. Morgan & Claypool, San Rafael, CA (2016)

6. Driessens, K., Džeroski, S.: Integrating guidance into relational reinforcement learning. *Machine Learning* **57**(3), 271–304 (2004)
7. Dzeroski, S., Raedt, L.D., Blockeel, H.: Relational reinforcement learning. In: *Proceedings of the Fifteenth International Conference on Machine Learning*, p. 136–143. ICML '98, Morgan Kaufmann Publishers Inc., San Francisco, CA, USA (1998)
8. Ernst, D., Geurts, P., Wehenkel, L.: Tree-based batch mode reinforcement learning. *Journal of Machine Learning Research* **6**(18), 503–556 (2005), <http://jmlr.org/papers/v6/ernst05a.html>
9. Esteva, F., Godo, L.: Monoidal t-norm based logic:towards a logic for left-continuous t-norms. *Fuzzy Sets and Systems* **124**(3), 271–288 (2001). [https://doi.org/https://doi.org/10.1016/S0165-0114\(01\)00098-7](https://doi.org/https://doi.org/10.1016/S0165-0114(01)00098-7), <https://www.sciencedirect.com/science/article/pii/S0165011401000987>, fuzzy Logic
10. Evans, R., Grefenstette, E.: Learning explanatory rules from noisy data. *J. Artif. Int. Res.* **61**(1), 1–64 (jan 2018)
11. Fikes, R.E., Nilsson, N.J.: Strips: A new approach to the application of theorem proving to problem solving. *Artificial Intelligence* **2**(3), 189–208 (1971), <https://www.sciencedirect.com/science/article/pii/0004370271900105>
12. Frosst, N., Hinton, G.E.: Distilling a neural network into a soft decision tree. *CoRR* **abs/1711.09784** (2017), <http://arxiv.org/abs/1711.09784>
13. Garg, S., Bajpai, A., et al.: Size independent neural transfer for rddl planning. In: *Proceedings of the International Conference on Automated Planning and Scheduling*. vol. 29, pp. 631–636 (2019)
14. Garg, S., Bajpai, A., et al.: Symbolic network: generalized neural policies for relational mdps. In: *International Conference on Machine Learning*. pp. 3397–3407. PMLR (2020)
15. Gelfond, M., Lifschitz, V.: Action languages. *Electronic Transactions on Artificial Intelligence* **3**, 195–210 (1998), <http://www.cs.utexas.edu/users/ai-lab?ge198>
16. Ghallab, M., Howe, A., Knoblock, C., Mcdermott, D., Ram, A., Veloso, M., Weld, D., Wilkins, D.: PDDL—The Planning Domain Definition Language (1998), <http://citeseerx.ist.psu.edu/viewdoc/summary?doi=10.1.1.37.212>
17. Gilpin, L.H., Bau, D., Yuan, B.Z., Bajwa, A., Specter, M.A., Kagal, L.: Explaining explanations: An approach to evaluating interpretability of machine learning. *CoRR* **abs/1806.00069** (2018), <http://arxiv.org/abs/1806.00069>
18. Graves, A., Wayne, G., Danihelka, I.: Neural turing machines (2014), <http://arxiv.org/abs/1410.5401>, cite arxiv:1410.5401
19. Gulwani, S., Harris, W.R., Singh, R.: Spreadsheet data manipulation using examples. *Commun. ACM* **55**(8), 97–105 (aug 2012), <https://doi.org/10.1145/2240236.2240260>
20. Gulwani, S., Polozov, O., Singh, R.: Program synthesis. *Foundations and Trends® in Programming Languages* **4**(1-2), 1–119 (2017), <http://dx.doi.org/10.1561/2500000010>
21. Gupta, S., Hazra, R., Dukkupati, A.: Networked multi-agent reinforcement learning with emergent communication. *arXiv preprint arXiv:2004.02780* (2020)
22. Iyer, R., Li, Y., Li, H., Lewis, M., Sundar, R., Sycara, K.: Transparency and explanation in deep reinforcement learning neural networks. In: *Proceedings of the 2018 AAAI/ACM Conference on AI, Ethics, and Society*. p. 144–150. AIES '18, Association for Computing Machinery, New York, NY, USA (2018), <https://doi.org/10.1145/3278721.3278776>

23. Jang, E., Gu, S., Poole, B.: Categorical reparameterization with gumbel-softmax. In: 5th International Conference on Learning Representations, ICLR 2017, Toulon, France, April 24-26, 2017, Conference Track Proceedings. p. 0. OpenReview.net, Palais des Congrès Neptune, Toulon, France (2017), <https://openreview.net/forum?id=rkE3y85ee>
24. Janisch, J., Pevný, T., Lisý, V.: Symbolic relational deep reinforcement learning based on graph neural networks. arXiv preprint arXiv:2009.12462 (2020)
25. Jiang, Z., Luo, S.: Neural logic reinforcement learning. In: Proceedings of the 36th International Conference on Machine Learning. Proceedings of Machine Learning Research, vol. 97, pp. 3110–3119. PMLR, Long Beach, USA (09–15 Jun 2019), <https://proceedings.mlr.press/v97/jiang19a.html>
26. Kersting, K., Driessens, K.: Non-parametric policy gradients: A unified treatment of propositional and relational domains. In: Proceedings of the 25th International Conference on Machine learning. pp. 456–463 (2008)
27. Kersting, K., Otterlo, M.V., De Raedt, L.: Bellman goes relational. In: Proceedings of the twenty-first international conference on Machine learning. p. 59 (2004)
28. Khoshafian, S.N., Copeland, G.P.: Object identity. ACM SIGPLAN Notices **21**(11), 406–416 (1986)
29. Kipf, T.N., Welling, M.: Semi-Supervised Classification with Graph Convolutional Networks. In: Proceedings of the 5th International Conference on Learning Representations. ICLR '17 (2017), <https://openreview.net/forum?id=SJU4ayYg1>
30. Kokel, H., Manoharan, A., Natarajan, S., Ravindran, B., Tadepalli, P.: Reprel: Integrating relational planning and reinforcement learning for effective abstraction. In: Proceedings of the International Conference on Automated Planning and Scheduling. vol. 31, pp. 533–541 (2021)
31. Krajzewicz, D., Erdmann, J., Behrisch, M., Bieker, L.: Recent development and applications of sumo-simulation of urban mobility. International journal on advances in systems and measurements **5**(3&4) (2012)
32. Lamb, L.C., Garcez, A.d., Gori, M., Prates, M.O., Avelar, P.H., Vardi, M.Y.: Graph neural networks meet neural-symbolic computing: A survey and perspective. In: Bessiere, C. (ed.) Proceedings of the Twenty-Ninth International Joint Conference on Artificial Intelligence, IJCAI-20. pp. 4877–4884. International Joint Conferences on Artificial Intelligence Organization, Yokohama, Japan (7 2020), <https://doi.org/10.24963/ijcai.2020/679>, survey track
33. Lee, J.D., See, K.A.: Trust in automation: Designing for appropriate reliance. Human factors **46** 1, 50–80 (2004)
34. Liu, G., Schulte, O., Zhu, W., Li, Q.: Toward interpretable deep reinforcement learning with linear model u-trees. In: ECML/PKDD (2018)
35. Lloyd, J.W.: Foundations of Logic Programming. Springer-Verlag, Berlin, Heidelberg (1984)
36. Lyu, D., Yang, F., Liu, B., Gustafson, S.: Sdrl: Interpretable and data-efficient deep reinforcement learning leveraging symbolic planning. In: Proceedings of the Thirty-Third AAAI Conference on Artificial Intelligence and Thirty-First Innovative Applications of Artificial Intelligence Conference and Ninth AAAI Symposium on Educational Advances in Artificial Intelligence. AAAI'19/IAAI'19/EAAI'19, AAAI Press, Honolulu, Hawaii, USA (2019), <https://doi.org/10.1609/aaai.v33i01.33012970>
37. Marra, G., Giannini, F., Diligenti, M., Maggini, M., Gori, M.: T-norms driven loss functions for machine learning. arXiv: Artificial Intelligence (2019)
38. Martínez, D., Alenya, G., Torras, C.: Relational reinforcement learning with guided demonstrations. Artificial Intelligence **247**, 295–312 (2017)

39. Muggleton, S., De Raedt, L.: Inductive logic programming: Theory and methods. *Journal Of Logic Programming* **19**(20), 629–679 (1994)
40. Nau, D., Ghallab, M., Traverso, P.: *Automated Planning: Theory & Practice*. Morgan Kaufmann Publishers Inc., San Francisco, CA, USA (2004)
41. Payani, A., Fekri, F.: Incorporating relational background knowledge into reinforcement learning via differentiable inductive logic programming. arXiv preprint arXiv:2003.10386 (2020)
42. Quinlan, J.R.: Learning logical definitions from relations. *Mach. Learn.* **5**(3), 239–266 (sep 1990). <https://doi.org/10.1023/A:1022699322624>, <https://doi.org/10.1023/A:1022699322624>
43. Schkufza, E., Sharma, R., Aiken, A.: Stochastic superoptimization. In: *Proceedings of the Eighteenth International Conference on Architectural Support for Programming Languages and Operating Systems*. p. 305–316. ASPLOS '13, Association for Computing Machinery, New York, NY, USA (2013), <https://doi.org/10.1145/2451116.2451150>
44. Silva, A., Gombolay, M., Killian, T., Jimenez, I., Son, S.H.: Optimization methods for interpretable differentiable decision trees applied to reinforcement learning. In: Chiappa, S., Calandra, R. (eds.) *Proceedings of the Twenty Third International Conference on Artificial Intelligence and Statistics. Proceedings of Machine Learning Research*, vol. 108, pp. 1855–1865. PMLR, Palermo, Italy (26–28 Aug 2020), <https://proceedings.mlr.press/v108/silva20a.html>
45. Singh, R., Kohli, P.: Ap: Artificial programming. In: *2nd Summit on Advances in Programming Languages (SNAPL 2017)* (April 2017), <https://www.microsoft.com/en-us/research/publication/ap-artificial-programming/>
46. Solar-Lezama, A.: *Program Synthesis by Sketching*. Ph.D. thesis, University of California at Berkeley, USA (2008), <https://dl.acm.org/doi/10.5555/1714168.aAI3353225>
47. Stowers, K., Kasdaglis, N., Newton, O.B., Lakhmani, S.G., Wohleber, R.W., Chen, J.Y.: Intelligent agent transparency. *Proceedings of the Human Factors and Ergonomics Society Annual Meeting* **60**, 1706 – 1710 (2016)
48. Summers, P.D.: A methodology for lisp program construction from examples. *J. ACM* **24**(1), 161–175 (jan 1977), <https://doi.org/10.1145/321992.322002>
49. Tadepalli, P., Givan, R., Driessens, K.: Relational reinforcement learning: An overview. In: *Proceedings of the ICML'04 Workshop on Relational Reinforcement Learning* (2004)
50. Udupa, A., Raghavan, A., Deshmukh, J.V., Mador-Haim, S., Martin, M.M., Alur, R.: Transit: Specifying protocols with concolic snippets. *SIGPLAN Not.* **48**(6), 287–296 (jun 2013), <https://doi.org/10.1145/2499370.2462174>
51. de Visser, E.J., Cohen, M., Freedy, A., Parasuraman, R.: A design methodology for trust cue calibration in cognitive agents. In: Shumaker, R., Lackey, S. (eds.) *Virtual, Augmented and Mixed Reality. Designing and Developing Virtual and Augmented Environments*. pp. 251–262. Springer International Publishing, Cham (2014)
52. Williams, R.J.: Simple statistical gradient following algorithms for connectionist reinforcement learning. *Machine Learning* **8**, 229–256 (1992), <https://doi.org/10.1007/BF00992696>
53. Xu, J., Zhang, Z., Friedman, T., Liang, Y., Broeck, G.: A semantic loss function for deep learning with symbolic knowledge. In: *International conference on machine learning*. pp. 5502–5511. PMLR (2018)
54. Xu, R., Wunsch, D.: Survey of clustering algorithms. *IEEE Transactions on Neural Networks* **16**(3), 645–678 (2005). <https://doi.org/10.1109/TNN.2005.845141>

55. Yang, F., Lyu, D., Liu, B., Gustafson, S.: Peorl: Integrating symbolic planning and hierarchical reinforcement learning for robust decision-making. In: Proceedings of the 27th International Joint Conference on Artificial Intelligence. p. 4860–4866. IJCAI'18, AAAI Press, Stockholm, Sweden (2018)
56. Zambaldi, V.F., Raposo, D., Santoro, A., Bapst, V., Li, Y., Babuschkin, I., Tuyls, K., Reichert, D.P., Lillicrap, T.P., Lockhart, E., Shanahan, M., Langston, V., Pascanu, R., Botvinick, M., Vinyals, O., Battaglia, P.W.: Relational deep reinforcement learning. CoRR **abs/1806.01830** (2018), <http://arxiv.org/abs/1806.01830>
57. Zhang, K., Yang, Z., Liu, H., Zhang, T., Basar, T.: Fully decentralized multi-agent reinforcement learning with networked agents. In: International Conference on Machine Learning. pp. 5872–5881. PMLR (2018)

Appendix for “Deep Explainable Relational Reinforcement Learning: A Neuro-Symbolic Approach”

8 Semantic Constraints

Following are the semantic constraints used for each setup

The Countdown Game.

$$\begin{aligned} false &\leftarrow goal(X), goal(Y) & false &\leftarrow less(X, Y), less(Y, X) \\ less(X, Z) &\leftarrow less(X, Y), less(Y, Z) & false &\leftarrow acc(X), acc(Y) \\ false &\leftarrow curr(X), curr(Y) \end{aligned}$$

Blocks World Manipulation.

$$\begin{aligned} false &\leftarrow isFloor(X), isFloor(Y) & false &\leftarrow on(X, Y), on(Y, X) \\ false &\leftarrow on(X, Y), on(X, Z) & false &\leftarrow top(X), on(Y, X) \\ false &\leftarrow top(Y), isFloor(Y) & false &\leftarrow goal(X, Y), goal(Y, X) \end{aligned}$$

DoorKey Minigrid.

$$\begin{aligned} false &\leftarrow carrying(X), notcarrying \\ samecolor(X, Y) &\leftarrow samecolor(Y, Z), samecolor(Z, X) \\ samecolor(X, Y) &\leftarrow samecolor(Y, X) \\ false &\leftarrow carrying(X), carrying(Y) \\ false &\leftarrow locked(X), unlocked \end{aligned}$$

Traffic

$$\begin{aligned} between(X, Y, Z) &\leftarrow between(X, Z, Y) \\ false &\leftarrow highest(X), highest(Y), highest(Z) \end{aligned}$$

Gridworld Game

$$false \leftarrow curr(X, Y), curr(Y, X) \quad false \leftarrow succ(X, Y), succ(Y, X)$$

9 Computation Time comparison

See Figure 4 for run-time comparison of DERRL and NLRL for Gridworld, DoorKey, and Traffic domains. Additionally, as shown in Figure 5, without the use of semantic constraints, the convergence in DERRL is slower and the learned rules are redundant.

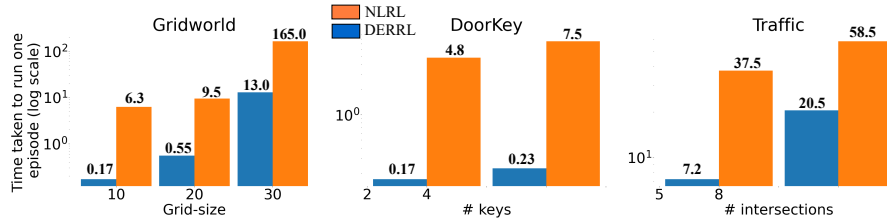


Fig. 4: Comparison of run-time per episode of DERRL and NLRL with problem scaling: From left to right: Gridworld (grid-size), DoorKey (number of keys), Traffic (number of intersections). The Y-axis is represented in log scale. The plots show that time taken per episode is significantly higher for NLRL, compared to DERRL.

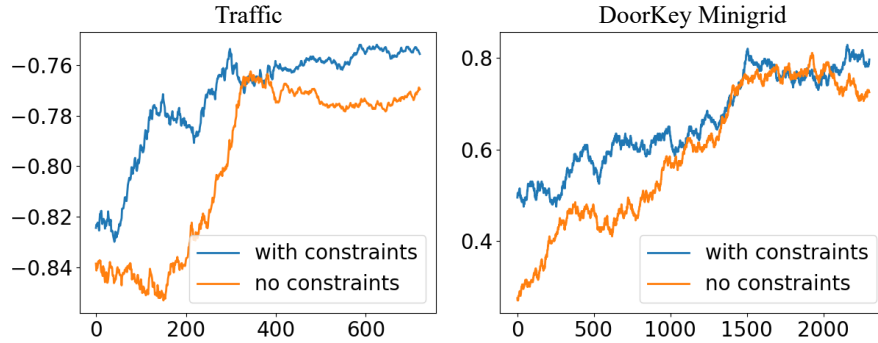


Fig. 5: Ablations on semantic constraints. Figure shows how the use of semantic constraints lead to faster convergence in the Traffic (Left) and the DoorKey Minigrid (Right) domains.

10 Analogies with Program Synthesis

In many ways, program synthesis techniques exhibit the same challenges as that of interpretable policy learning, wherein, programs generated using neural methods cannot generalize to new problems [18,45], and symbolic methods employing search-based methods are faced with the curse of dimensionality [46,43,50]. Our exploratory study indicates that our rule generation framework is closely related to the paradigm of rule-based program synthesis [19,1]. The specification here is – one needs to find a sequence of instructions (a program or a policy) that transforms the given state into a target state. However, in program synthesis, the instructions are usually deterministic, while in RRL they can be stochastic. Note, that DERRL selects at every time step the next action and moves to the next position and iterates. Although DERRL uses non-recursive rules, the

learned policies are applied iteratively, which results in programs as shown in Figure 6.

Countdown Game	Gridworld	DoorKey Minigrid
<pre>while goal != acc: if acc ≤ goal: add() elif acc ≥ goal: sub() else: null()</pre>	<pre>if dir in [north, northeast, northwest] up elif dir in [south, southeast, southwest] down elif dir == east right else: left</pre>	<pre>if notcarrying: if door(Y) and samecolor(X, Y): pickup(X) elif locked(X): if key(Z) and samecolor(X, Z): open(X) elif unlocked: if goal(X): goto(X)</pre>
Traffic	Blocksworld	
<pre>if highest(X): if intesection(Y) and interseccion(Z): if between(X, Y, Z): green()</pre>	<pre>while not top(a) and not top(b): unstack() move(a, b)</pre>	

Fig. 6: Programs for different environments: [Row 1]: from left to right, Countdown Game, Gridworld, DoorKey Minigrid. [Row 2]: from left to right, Traffic and Blocksworld.

11 Fuzzy Conjunction Operators

A fuzzy conjunction operator $*$: $[0, 1]^e \mapsto [0, 1]$ must satisfy the following conditions on a t-norm [9] (here, e is the number of atoms in the rule body):

- commutativity: $a * b = b * a$
- associativity: $(a * b) * c = a * (b * c)$
- monotonicity:
 1. $a_1 \leq a_2$ implies $a_1 * b \leq a_2 * b$
 2. $b_1 \leq b_2$ implies $a * b_1 \leq a * b_2$
- unit:
 1. $a * 1 = a$
 2. $a * 0 = 0$

The operators that satisfy the aforementioned conditions are:

- Godel t-norm: $a * b := \min(a, b)$
- Lukasiewicz t-norm $\top_{\text{Luk}}(a, b) := \max\{0, a + b - 1\}$
- Product t-norm: $a * b := a \cdot b$ (ordinary product of real numbers)

Lukasiewicz t-norm was experimentally found to perform better than other alternatives.

Proposition 1 *More generally, given a vector $\mathbf{y} \in [0, 1]^n$, Lukasiewicz t-norm*

$$\top_{Luk}\mathbf{y} := \max(0, \langle \mathbf{y}, \mathbb{1} \rangle - n + 1) \quad (1)$$

Proof. . We prove it using mathematical induction.

Base Case: For $\mathbf{y} = [a, b]$, eq. 1 is clearly true.

$$\top_{Luk}(a, b) := \max(0, a + b - 2 + 1)$$

Inductive Step: Let, $\top_{Luk}\mathbf{y}$ hold for $\mathbf{y} \in [0, 1]^k$. We denote it as,

$$\top_{Luk}\mathbf{y} := \max(0, \langle \mathbf{y}, \mathbb{1} \rangle - k + 1) \quad (2)$$

Now let $\tilde{\mathbf{y}} \in [0, 1]^{k+1}$. Using the associativity property:

$$\begin{aligned} \top_{Luk}\tilde{\mathbf{y}} &:= \max(0, \top_{Luk}\mathbf{y} + y_{k+1} - 1) \\ &:= \max(0, \max(0, \langle \mathbf{y}, \mathbb{1} \rangle - k + 1) + y_{k+1} - 1) \end{aligned}$$

– Case 1: $\langle \mathbf{y}, \mathbb{1} \rangle > (k - 1)$. It follows that $\max(0, \langle \mathbf{y}, \mathbb{1} \rangle - k + 1) = \langle \mathbf{y}, \mathbb{1} \rangle - k + 1$

$$\begin{aligned} \top_{Luk}\tilde{\mathbf{y}} &:= \max(0, \langle \mathbf{y}, \mathbb{1} \rangle - k + 1 + y_{k+1} - 1) \\ &:= \max(0, y_1 + \dots + y_k - k + 1 + y_{k+1} - 1) \\ &:= \max(0, \langle \tilde{\mathbf{y}}, \mathbb{1} \rangle - (k + 1) - 1) \end{aligned}$$

Thus, eqn. 1 is true.

– Case 2: $\langle \mathbf{y}, \mathbb{1} \rangle \leq (k - 1)$. It follows that $\max(0, \langle \mathbf{y}, \mathbb{1} \rangle - k + 1) = 0$

$$\begin{aligned} \top_{Luk}\tilde{\mathbf{y}} &:= \max(0, y_{k+1} - 1) \\ &:= 0 \quad \text{since } y_{k+1} \in [0, 1] \end{aligned}$$

Also, $\langle \mathbf{y}, \mathbb{1} \rangle \leq (k - 1) \implies \langle \tilde{\mathbf{y}}, \mathbb{1} \rangle \leq k$ since $y_{k+1} \in [0, 1]$.

\therefore from eqn. 1, $\top_{Luk}\tilde{\mathbf{y}} := 0$

12 Code

All models were run on CPU nodes. The codes will be made available soon.